frontiers in Oncology

ORIGINAL RESEARCH
published: 26 May 2021
doi: 10.3389/fonc.2021.573798

Brain Microstructural Changes Associated With Neurocognitive Outcome in Intracranial Germ Cell Tumor Survivors

Winnie Wan Yee Tso[1‡], Edward Sai Kam Hui[2†‡], Tatia Mei Chun Lee[3,4], Anthony Pak Yin Liu[1], Patrick Ip[1], Vince Vardhanabhuti[2], Kevin King Fai Cheng[5], Daniel Yee Tak Fong[6], Dorita Hue Fung Chang[3,7], Frederick Ka Wing Ho[8], Ka Man Yip[1], Dennis Tak Loi Ku[9], Daniel Ka Leung Cheuk[10], Chung Wing Luk[9], Ming Kong Shing[9], Lok Kan Leung[1], Pek Lan Khong[2] and Godfrey Chi-Fung Chan[1]*

[1] Department of Paediatrics and Adolescent Medicine, Queen Mary Hospital, Li Ka Shing (LKS) Faculty of Medicine, The University of Hong Kong, Hong Kong, Hong Kong, [2] Department of Diagnostic Radiology, Queen Mary Hospital, Li Ka Shing Faculty of Medicine, The University of Hong Kong, Hong Kong, Hong Kong, [3] State Key Laboratory of Brain and Cognitive Sciences, The University of Hong Kong, Hong Kong, Hong Kong, [4] Laboratory of Neuropsychology, The University of Hong Kong, Hong Kong, Hong Kong, [5] Department of Neurosurgery, Hong Kong Children's Hospital, Hong Kong, Hong Kong, [6] School of Nursing, The University of Hong Kong, Hong Kong, Hong Kong, [7] Department of Psychology, The University of Hong Kong, Hong, Kong, Hong Kong, [8] Institute of Health and Wellbeing, University of Glasgow, Glasgow, United Kingdom, [9] Department of Oncology, Hong Kong Children's Hospital, Hong Kong, Hong Kong, [10] Department of Paediatrics and Adolescent Medicine, Hong Kong Children's Hospital, Hong Kong, Hong Kong

Background: Childhood intracranial germ cell tumor (GCT) survivors are prone to radiotherapy-related neurotoxicity, which can lead to neurocognitive dysfunctions. Diffusion kurtosis imaging (DKI) is a diffusion MRI technique that is sensitive to brain microstructural changes. This study aimed to investigate the association between DKI metrics versus cognitive and functional outcomes of childhood intracranial GCT survivors.

Methods: DKI was performed on childhood intracranial GCT survivors (n = 20) who had received cranial radiotherapy, and age and gender-matched healthy control subjects (n = 14). Neurocognitive assessment was performed using the Hong Kong Wechsler Intelligence Scales, and functional assessment was performed using the Lansky/Karnofsky performance scales (KPS). Survivors and healthy controls were compared using mixed effects model. Multiple regression analyses were performed to determine the effects of microstructural brain changes of the whole brain as well as the association between IQ and Karnofsky scores and the thereof.

Results: The mean Intelligence Quotient (IQ) of GCT survivors was 91.7 (95% CI 84.5 – 98.8), which was below the age-specific normative expected mean IQ (P = 0.013). The mean KPS score of GCT survivors was 85.5, which was significantly lower than that of controls (P < 0.001). Cognitive impairments were significantly associated with the presence of microstructural changes in white and grey matter, whereas functional impairments were mostly associated with microstructural changes in white matter.

OPEN ACCESS

Edited by:
Zaver Bhujwalla,
Johns Hopkins University,
United States

Reviewed by:
Kumar Pichumani,
Houston Methodist Research Institute,
United States
Khin Khin Tha,
Hokkaido University, Japan

***Correspondence:**
Godfrey Chi-Fung Chan
gcfchan@hku.hk

†Present address:
Edward Sai Kam Hui,
Department of Rehabilitative Science,
The Hong Kong Polytechnic
University, Hong Kong, Hong Kong

‡These authors share first authorship

Specialty section:
This article was submitted to
Cancer Imaging and
Image-directed Interventions,
a section of the journal
Frontiers in Oncology

Received: 19 June 2020
Accepted: 06 April 2021
Published: 26 May 2021

Citation:
Tso WWY, Hui ESK, Lee TMC,
Liu APY, Ip P, Vardhanabhuti V,
Cheng KKF, Fong DYT, Chang DHF,
Ho FKW, Yip KM, Ku DTL, Cheuk DKL,
Luk CW, Shing MK, Leung LK,
Khong PL and Chan GC-F (2021)
Brain Microstructural Changes
Associated With Neurocognitive
Outcome in Intracranial Germ Cell
Tumor Survivors.
Front. Oncol. 11:573798.
doi: 10.3389/fonc.2021.573798

There were significant correlations between IQ versus the mean diffusivity (MD) and mean kurtosis (MK) of specific white matter regions. The IQ scores were negatively correlated with the MD of extensive grey matter regions.

Conclusion: Our study identified vulnerable brain regions whose microstructural changes in white and grey matter were significantly associated with impaired cognitive and physical functioning in survivors of pediatric intracranial GCT.

Keywords: intracranial germ cell tumor, neurotoxicity, diffusion kurtosis imaging, brain microstructure, cognition, functional outcome

INTRODUCTION

Intracranial germ cell tumors (GCT), while rare in the West, are more common in Asia accounting for up to 15% of primary intracranial tumors in Asian children. Germinomas are the most common subtype of GCT. Despite of the excellent survival rate for intracranial GCT, the relatively large volumes and high doses of radiation required to treat intracranial GCT can impact neurocognitive and functional outcomes. Treatment-related neurotoxicity was shown to be particularly harmful to specific cognitive processes, such as executive functions (1, 2). Furthermore, a recent study reported that the intelligence quotient (IQ) of nearly 20% of pediatric intracranial GCT survivors was borderline or worse (3).

Because of the high survival rates of childhood intracranial GCT, there is growing concern over the long-term neurocognitive outcomes. Among the different types of intracranial germinomas, basal ganglia germinomas tended to result in the worst neurocognitive outcomes (4). It is believed that the deep grey matter of children is more susceptible to oxidative damage. Damage to the basal ganglia and deep brain nuclei can lead to cognitive impairment as well as loss of motor control (5). Majority of basal ganglia germinomas with poor neurocognitive outcomes were also associated with early cerebral atrophy (6). It was proposed that atrophy occurs as a result of tumor involvement of the internal capsule fibers or thalamic ganglion cells, with Wallerian degeneration and subsequent interruption of thalamocortical connections leading to detrimental effects on motor function and functional outcomes (7). It is thus conceivable that the cognitive and functional impairments in intracranial GCT survivors are likely due to both grey and white matter damage.

Numerous neuroimaging studies have investigated the association between brain changes and neurocognitive and functional outcomes in brain tumor survivors (8, 9). However, previous studies suggested that brain volume or volumetric white matter changes might be a poor predictor of neurocognitive deficits in the later life of cancer survivors (9–11). Conventional MRI methods might not be sensitive enough to identify changes that are predictive of neurocognitive dysfunction.

We have previously demonstrated that fractional anisotropy (FA), a diffusion metric commonly obtained from diffusion tensor imaging (DTI), correlated with the cognitive outcomes of medulloblastoma survivors (12, 13). Diffusion tensor imaging is a diffusion MRI technique that measures the diffusion of water molecules, a process that is very sensitive to tissue microstructural changes. Fractional anisotropy and mean diffusivity (MD) are the two most common diffusion metrics obtained from DTI. Notably, neurological/functional impairments were found to be more related to white matter injury, whereas cognitive impairments were associated with both white and grey matter injuries (14). So far, there have been no investigations on the relation between grey matter changes and cognitive outcomes in brain tumor survivors.

In the past few years, diffusional kurtosis imaging (DKI), an extension to DTI, has been shown to be more sensitive to microstructural changes in white and grey matter in adult neurological diseases such as stroke (15, 16), traumatic brain injury (17), and Alzheimer's disease (18). We therefore hypothesized that diffusion metrics obtained from DKI would be more sensitive to the white and grey matter changes of intracranial GCT survivors, and these metrics might be associated with functional and neurocognitive outcomes. The aim of this study was to investigate whether white and grey matter microstructural changes as measured by DKI were associated with functional and neurocognitive outcomes in childhood intracranial GCT survivors.

METHODS

We conducted a cross-sectional study to determine if changes in brain microstructure would correlate with the neurocognitive and functional outcomes of childhood intracranial GCT survivors with a history of cranial radiotherapy. This study was approved by the ethical committees of the Institutional Review Board of the University of Hong Kong and Hospital Authority Hong Kong West Cluster, Kowloon West and Kowloon Central Clusters, and New Territories East and New Territories West Clusters. Informed written consent was obtained from the parents of participants under the age of 18 years or from participants aged ≥ 18 years. Neurocognitive outcomes were assessed using the Full Scale Intelligence Quotient (FSIQ) and functional outcomes were assessed using Lansky/Karnofsky performance scales.

Subject Recruitment

We recruited all the survivors of childhood intracranial GCT over the past 20 years from the database of the Hong Kong Pediatric Hematology and oncology study group. Of the 62 GCT survivors, 25 completed the full assessments for this study. The remaining 37 survivors were either lost to follow-up due to

changes in contact details/moved abroad, or they declined to join the study due to refusal to have follow-up imaging/busy work or school schedule/not interested in joining the study. All of the participants completed treatment at least 1 year prior, were currently free of the primary disease, and were at least 6 years of age at the time of recruitment. Treatment of intracranial GCT was delivered according to a standardized protocol based on SFOP and COG experience (19, 20). Following the initial diagnosis by tissue biopsy or resection, patients with germinoma were treated by chemotherapy with either BEP (bleomycin, etoposide, cisplatin) or SFOP which consisted of alternated cycle of CE-IE (carboplatin, etoposide, ifosphamide). The dose and volume of radiotherapy was based on the response and site of involvement. Patients with non-germinomatous GCT received chemotherapy as above for six cycles followed by craniospinal radiotherapy and tumor boost. Reassessment by MRI was performed every other chemotherapy cycle and at the end of the treatment (3).

Age and gender-matched healthy children were recruited as controls from volunteers or patients undergoing brain MRI for clinical indications such as headaches, but were later confirmed to have no neurological deficits by clinical examination and MRI.

Data Acquisition

The MRI was performed using a 3.0 Tesla MRI Scanner (Achieva TX, Philips, Best, Netherland) with an 8-channel head coil. The DKI data were acquired using a Stejskal–Tanner diffusion-weighted spin echo echo-planar imaging sequence with the following parameters: two b values (1000 and 2000 s/mm^2), 32 diffusion-encoding directions, TR/TE = 2000/72 ms, FOV = 234 x 224 mm^2, acquisition matrix = 96 x 94, slice thickness = 3 mm (no gap), SENSE factor = 2 (along AP), number of averages = 2, and scan time = 12.8 minutes.

Whole-brain T1-weighted images were acquired using MPRAGE with the following parameters: TR/TE = 7/3.2 ms, flip angle = 8°, FOV = 224 x 224 x 167 mm^3, acquisition matrix = 224 x 224 x 167, and scan time = 2.7 minutes. Fluid-attenuated inversion recovery (FLAIR) sequence was also acquired with the following parameters: IR/TR/TE = 2800/9600/120 ms, FOV = 230 x 182 mm^2, acquisition matrix = 192 x 157, slice thickness = 2.5 mm, and scan time = 10.7 minutes.

Image Post-Processing

Brain parcellation: T1-weighted images were used to partition the brain into 90 cortical and subcortical regions based on the Automated anatomical labeling (AAL) atlas using Statistical Parametric Mapping (version 12; SPM12) (https://www.fil.ion.ucl.ac.uk/spm/software/spm12/) with the following steps: (1) DKI data (average of diffusion-weighted images along all diffusion directions) were first co-registered to T1-weighted images in anatomical space. (2) T1-weighted images were normalized to the ICBM 152 template in standard space. (3) The estimated transformation parameters were subsequently applied to the parametric map of diffusion metrics in anatomical space to ensure they were all in standard space for the subsequent region-of-interest analyses.

Diffusion metrics: The DKI data were first corrected in SPM for any misregistration caused by head motion and eddy currents. Diffusional Kurtosis Estimator (version 2.6; https://medicine.musc.edu/departments/centers/cbi/dki/dki-data-processing) was used to obtain diffusion metrics (21) including mean kurtosis (MK), MD and FA.

Region-based analysis: The diffusion metrics of all 90 cortical and subcortical regions from the AAL, and all major white matter tracts from the Johns Hopkins white matter atlas were measured from all subjects. Measurements were obtained by averaging the diffusion metrics from all the pixels within a given brain region. To avoid partial volume effects from non-brain pixels, the following thresholds were used: $0 < FA < 0.9$, $0.2 < MD < 3$ um^2/ms, and $0.3 < MK < 2$.

Neuropsychological Tests and Functional Outcomes

The neuropsychological assessments and functional outcomes were performed within 1 year of the MRI. Full scale IQ scores were obtained using the Hong Kong Wechsler Intelligence Scales for Children (WISC) for subjects aged under 16 years and the Wechsler Adult Intelligence Scale – Revised (WAIS-R) for subjects aged 16 years and over. Functional outcomes were assessed using the Lansky play-performance scales for subjects aged 6 to 15 years and Karnofsky performance scales (KPS) for subjects aged 16 years and over.

Statistical Analysis

Survivors and healthy controls were compared using mixed effects model to account for extra covariance within each matched pair. Multiple regression analyses were performed to determine the effects of microstructural brain changes of the whole brain as well as each segmental white and grey matter regions on IQ and Karnofsky scores with adjustment of sex, age, radiation dosage, length of time since treatment, and treatment methods. Separate regression analyses were performed for each diffusion MRI metric with each white and grey matter regions from the AAL atlas. Holm's sequential Bonferroni procedure was used to account for multiplicity due to multiple comparisons. All statistical analyses were performed using the computing environment R (R Development Core Team 2018). P-value < 0.05 was considered statistically significant.

RESULTS

Patients, Tumor Characteristics, and Treatment Modalities

All of the 25 GCT patients completed IQ tests and functional outcome assessment, but 5 of them failed the MRI examinations because of claustrophobia or technical problems and were excluded from the analyses. Therefore, 20 patients (**Table 1**) together with 14 age- and gender-matched healthy control subjects were included in the final analyses. Of the 20 survivors, 15 were male and five were female, with a median age at diagnosis of 14.4 years and average length of time since treatment of 6.5 years. There were 13 germinomatous germ cell tumor (GCT) survivors and 7 non-germinomatous germ cell tumor (NGGCT) survivors. Tumor locations included the suprasellar/sellar region (n = 7), basal ganglia (n = 5), pineal region (n = 4), bifocal regions (n = 3), and brainstem (n = 1). Six patients had surgical resection of the tumor,

chemotherapy and radiotherapy, whereas 14 had chemotherapy and radiotherapy only. The average total irradiation dose was 42.16 Gy (range 30 – 54 Gy). The average IQ score of GCT survivors was 91.7 (CI 84.5 – 98.8), which was below the age-specific normative expected IQ in the validated WISC IV or WAIS III ($P = 0.013$). The average KPS score of GCT survivors was 85.5, which was significantly lower than normal ($P < 0.001$). All clinical characteristics are summarized in **Table 1**.

Diffusion Metrics of White Matter

Compared to healthy controls, GCT survivors had significantly higher MD in the cingulum, fornix, uncinate fasciculus, superior fronto-occipital fasciculus, anterior limb of internal capsule, anterior and superior corona radiata, and the cerebral peduncle (**Figure 1A**, **Supplementary Table 1**). They had significantly lower MK in the cingulum, fornix, superior longitudinal fasciculus, anterior and superior corona radiate, and anterior limb of the internal capsule (**Figure 1B**). They also had significantly lower FA values in the cingulum, fornix, posterior corona radiata, posterior thalamic radiation, and anterior limb of the internal capsule (**Figure 1C**).

Diffusion Metrics of Grey Matter

Compared to healthy controls, GCT survivors had significantly higher MD in the anterior, middle and posterior cingulum, amygdala, frontal inferior triangularis, Heschl's gyrus, supramarginal gyrus, calcarine sulcus, superior and middle inferior temporal gyrus, precentral and postcentral gyrus, frontal inferior operculum, superior temporal pole, insula, fusiform, rolandic operculum, lingual gyrus, and cuneus (**Figure 1D**, **Supplementary Table 2**).

Relations Between Diffusion Metrics of the Whole Brain Versus IQ and KPS Scores

Lower IQ (**Table 2A**) and KPS (**Table 2B**) scores were associated with higher MD values in the white matter of the whole brain. No significant associations were found for the grey matter of the whole brain.

Relations Between IQ Scores and Diffusion Metrics of All Brain Regions in the AAL Atlas

For the white matter of GCT survivors, lower IQ scores were associated with higher MD values in the anterior limb of the internal capsule, superior fronto-occipital fasciculus, anterior corona radiata, uncinate fasciculus, cingulum, and the hippocampus; and lower IQ scores were associated with lower MK values in the superior fronto-occipital fasciculus. For the grey matter of GCT survivors, lower IQ scores were associated with higher MD values in the olfactory cortex, insula, caudate, Heschl's gyrus, parahippocampal gyrus, hippocampus, anterior cingulum, frontal inferior operculum, middle and superior temporal gyrus, middle and superior frontal orbital gyrus, cuneus, and precentral gyrus. All results are summarized in **Table 3A**.

Relations Between KPS Scores and Diffusion Metrics of All Brain Regions in the AAL Atlas

For the white matter of GCT survivors, KPS scores were negatively correlated with MD and positively correlated with FA and MK in the cerebral peduncle, superior longitudinal fasciculus, external capsule, and posterior limb of the internal capsule. Similar associations between KPS scores and MD were found in the superior and posterior corona radiata, and

TABLE 1 | Clinical Characteristics of GCT survivors.

Subject number	Sex	Age at diagnosis (years)	Length of time since treatment (years)	Types of germinoma	Tumor Loci	Size of GCT (largest length in cm)	Presence of hydrocephalus at presentation	Treatment	Total RT dosage (Gy)	RT field CSI + tumor boost dose (Gy)
1	M	11.7	9.3	GCT	Basal ganglia	0.7	No	C + RT	30.6	CSI (21.6) + TB (9)
2	M	15.1	10.9	NGGCT	Basal ganglia	3.0	No	C + RT	50.0	IFRT
3	M	8.8	1.2	NGGCT	Pineal	1.1	Yes	C + RT	46.8	CSI (30.6) + TB (16.2)
4	M	17.9	3.1	GCT	Others - Bifocal	2.3	No	C + RT	30.0	WVRT + TB
5	M	9.7	8.3	GCT	Basal ganglia	3.0	No	C + RT	50.4	WVRT + TB
6	F	10.7	5.3	NGGCT	Sellar/suprasellar	3.9	No	S, C + RT	54.0	CSI (36) + TB (18)
7	M	17.2	6.8	GCT	Pineal	0.9	Yes	C + RT	30.0	CSI (22.5) + TB (7.5)
8	F	17.5	6.5	GCT	Sellar/suprasellar	3.1	No	S, C + RT	36.0	WVRT + TB
9	F	15.8	3.2	NGGCT	Sellar/suprasellar	2.4	No	S, C + RT	54.0	CSI (36) + TB (18)
10	M	17.3	9.7	GCT	Sellar/suprasellar	1.4	No	C + RT	48.0	WBRT
11	M	13.8	12.2	GCT	Basal ganglia	6.0	No	C + RT	52.2	WBRT
12	F	7.7	7.3	NGGCT	Others - Bifocal	4.2	No	C + RT	45.0	CSI (24) + TB (21)
13	F	9.8	6.2	GCT	Sellar/suprasellar	1.0	No	C + RT	45.0	WVRT + TB
14	M	15.2	9.8	GCT	Pineal	2.7	Yes	C + RT	45.5	CSI (25.5) + TB (20)
15	M	10.9	6.1	GCT	Pineal	2.0	Yes	S, C + RT	45.0	WBRT
16	M	16.7	1.3	GCT	Sellar/suprasellar	4.1	No	C + RT	36.0	WBRT
17	M	17.5	2.5	NGGCT	Others - Brainstem	3.3	No	S, C + RT	54.0	CSI (36) + TB (18)
18	M	10.8	8.2	NGGCT	Sellar/suprasellar	1.3	No	S, C + RT	30.0	WVRT + TB
19	M	17.3	9.7	GCT	Others - Bifocal	4.2	No	C + RT	30.6	CSI (23.4) + TB (7.2)
20	M	10.9	1.8	NGGCT	Basal ganglia	3.5	No	C + RT	54.0	WVRT + IFRT

C, chemotherapy; S, surgery; RT, radiotherapy; GCT, germ cell tumors; CSI, cranial spinal irradiation; IFRT, involved field radiotherapy; WBRT, whole brain radiotherapy; WVRT, whole ventricular radiotherapy; TB, tumor boost.

GCT, Germ Cell Tumor; NGGCT, Nongerminomatous Germ Cell Tumor.

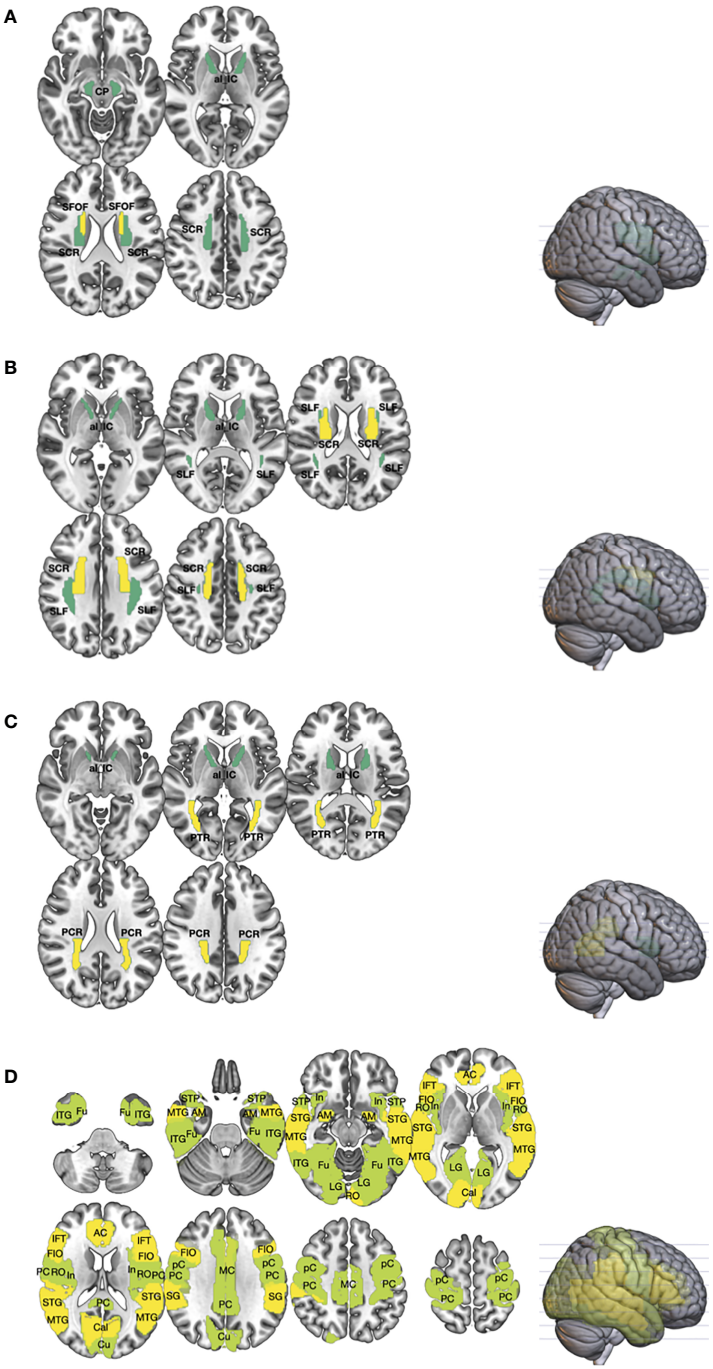

FIGURE 1 | The differences in the white (WM; **(A–C)** and gray matters (GM; **(D)** between germ cell tumor (GCT; n = 20) survivors and healthy age, sex-matched controls (n = 14) were investigated using diffusion metrics, namely mean diffusivity (MD), fractional anisotropy (FA), and mean kurtosis (MK), obtained from diffusional kurtosis imaging (DKI). Region-of-interest (ROI) measurement of the cortical and subcortical regions, from the Automated anatomical labeling (AAL) atlas, and major WM tracts, from the Johns Hopkins white matter atlas, were performed. The brain regions that showed statistically significant difference in diffusion metrics between GCT and healthy controls were shown ($P < 0.01$ in yellow; $P < 0.05$ in green). As compared to healthy controls, ROI analyses of the WM showed that the MD **(A)** of GCT survivors in the cerebral peduncle (CP), superior corona radiata (SCR), anterior limb of internal capsule (al_IC), and superior fronto-occipital fasciculus (SFOF) were higher; the MK **(B)** in the superior longitudinal fasciculus (SLF), SCR, and al_IC were lower; and the FA **(C)** in the posterior corona radiata (PCR), posterior thalamic radiation (PTR), and ac_IC were lower. Region-of-interest analysis of the GM **(D)** showed that the MD of GCT in fusiform (Fu), inferior temporal gyrus (ITG), middle temporal gyrus (MTG), superior temporal pole (STP), superior temporal gyrus (STG), amygdala (AM), insular (In), lingual gyrus (LG), rolandic operculum (RO), anterior cingulum (AC), middle cingulum (MC), posterior cingulum (PC), calcarine (Cal), cuneus (Cu), precentral gyrus (pC), postcentral gyrus (PC), supramarginal gyrus (SG), frontal inferior operculum (FIO), and inferior frontal triangularis (IFT) were significantly higher than those of healthy control.

TABLE 2A | Multiple regression analysis of the relationships between IQ and diffusion metrics of the whole brain.

Regions	Effect	95% CI	*P*
IQ – White matter MD			
Whole brain	-79.66	(-153.66, -5.65)	0.040
IQ – White matter MK			
Whole brain	106.37	(-13.57, 226.32)	0.084
IQ – Grey matter MD			
Whole brain	-63.74	(-119.72, -7.75)	0.119

MD, mean diffusivity; MK, mean kurtosis.

TABLE 2B | Multiple regression analysis of the relationships between Karnofsky score and diffusion metrics of the whole brain.

Regions	Effect	95% CI	*P*
Karnofsky score – White matter MD			
Whole brain	-84.78	(-149.67, -19.88)	0.017
Karnofsky score – White matter MK			
Whole brain	105.27	(-6.44, 216.88)	0.069
Karnofsky score – White matter FA			
Whole brain	181.93	(1.37, 362.49)	0.054
Karnofsky score – Grey matter MD			
Whole brain	-27.99	(-87.7, 31.73)	0.343

MD, mean diffusivity; MK, mean kurtosis; FA, fractional anisotropy.

retrolenticular part of the internal capsule. Similar associations between KPS scores and MK were found in the posterior and superior corona radiata, uncinate fasciculus, and superior fronto-occipital fasciculus. For the grey matter of GCT survivors, KPS scores were negatively correlated with MD in the pallidum, putamen, thalamus, rolandic operculum, and inferior temporal gyrus. All results are summarized in **Table 3B**.

TABLE 3A | Multiple regression analysis of the relationships between IQ and diffusion metrics of all brain regions in the AAL atlas.

Regions	Effect	95% CI	*P*
IQ – White matter MD			
Anterior limb of internal capsule	-71.83	(-31.02, -112.65)	<0.01
Superior fronto-occipital fasciculus	-34.14	(-13, -55.28)	<0.01
Uncinate fasciculus	-56.25	(-18.02, -94.48)	<0.01
Anterior corona radiata	-115.27	(-33.36, -197.19)	<0.05
Cingulum cingulate	-116.68	(-10.15, -223.21)	<0.05
Cingulum hippocampus	-50.34	(-1.74, -98.95)	<0.05
IQ – White matter MK			
Superior fronto-occipital fasciculus	73.37	(122.1, 24.64)	<0.01
IQ – Grey matter MD			
Heschl's gyrus	-41.04	(-14.58, -67.5)	<0.01
Insula	-64.02	(-22.2, -105.85)	<0.01
Parahippocampal gyrus	-70.34	(-24.28, -116.39)	<0.01
Caudate	-27.81	(-7.5, -48.13)	<0.05
Olfactory	-42.41	(-10.11, -74.71)	<0.05
Anterior cingulum	-71.1	(-16.75, -125.44)	<0.05
Hippocampus	-29.31	(-5.25, -53.36)	<0.05
Middle frontal orbital gyrus	-58.83	(-9.44, -108.23)	<0.05
Precentral gyrus	-53.16	(-8.26, -98.06)	<0.05
Frontal inferior operculum	-55.91	(-8.24, -103.57)	<0.05
Cuneus	-41.52	(-4.45, -78.6)	<0.05
Superior temporal gyrus	-45.72	(-2.67, -88.77)	<0.05
Superior frontal orbital gyrus	-38.18	(-1.83, -74.54)	<0.05
Middle temporal gyrus	-74.86	(-3.17, -146.55)	<0.05

MD, mean diffusivity; MK, mean kurtosis.

DISCUSSION

We have successfully demonstrated using diffusional kurtosis imaging that there were extensive microstructural changes in the grey and white matter of intracranial GCT survivors with a history of cranial irradiation when compared to healthy controls. The majority of these changes occurred in brain regions related to cognition and motor functions. Our study provides evidence that these extensive microstructural changes might underlie deficits in cognitive and motor functions, as well as problems with sensory processing. Our study also demonstrated that it is important to look at the microstructural changes of individual brain regions rather than just looking at the whole brain. Brain regions affected by the tumor or focal radiotherapy will be prone to more severe microstructural damages. Therefore, despite of the lack of association between IQ or KPS scores and microstructural changes in the whole brain grey matter, we found significant associations between the microstructural changes of specific grey matter regions and the IQ and KPS scores, which reflect cognitive and functional outcomes respectively.

TABLE 3B | Multiple regression analysis of the relationships between Karnofsky score and diffusion metrics of all brain regions in the AAL atlas.

Regions	Effect	95% CI	*P*
Karnofsky score – White matter MD			
Cerebral peduncle	-40.59	(-15.8, -65.38)	<0.01
Superior corona radiata	-84.7	(-28.04, -141.37)	<0.01
Posterior limb of internal capsule	-47.57	(-13.94, -81.2)	<0.01
Posterior corona radiata	-69.64	(-17.34, -121.94)	<0.05
Retrolenticular part of internal capsule	-50.61	(-12.44, -88.78)	<0.05
External capsule	-54.93	(-9.4, -100.46)	<0.05
Superior longitudinal fasciculus	-67.26	(-9.26, -125.27)	<0.05
Karnofsky score – White matter MK			
Superior longitudinal fasciculus	96.26	(173.9, 18.61)	<0.05
Cerebral peduncle	66.64	(122.41, 10.87)	<0.05
Posterior corona radiata	91.83	(169.67, 13.98)	<0.05
External capsule	127.46	(237.96, 16.97)	<0.05
Superior corona radiata	83.21	(155.57, 10.84)	<0.05
Uncinate fasciculus	94.75	(179.01, 10.48)	<0.05
Posterior limb of internal capsule	58.17	(112.56, 3.78)	<0.05
Superior fronto-occipital fasciculus	47.1	(91.38, 2.82)	<0.05
Karnofsky score – White matter FA			
Retrolenticular part of internal capsule	143.8	(233.52, 54.08)	<0.01
External capsule	175.26	(295.97, 54.55)	<0.01
Posterior limb of internal capsule	96.49	(172.27, 20.72)	<0.05
Uncinate fasciculus	111.13	(199.23, 23.02)	<0.05
Cerebral peduncle	97.69	(175.68, 19.7)	<0.05
Posterior thalamic radiation	156.4	(284.46, 28.34)	<0.05
Superior longitudinal fasciculus	168.56	(308.32, 28.79)	<0.05
Fornix	106.65	(196.4, 16.9)	<0.05
Karnofsky score – Grey matter MD			
Pallidum	-37.01	(-9.83, -64.2)	<0.05
Putamen	-57.12	(-11.58, -102.66)	<0.05
Thalamus	-39.31	(-7.17, -71.45)	<0.05
Rolandic operculum	-38.88	(-2.93, -74.82)	<0.05
Inferior temporal gyrus	-72.11	(-1.85, -142.37)	<0.05

MD, mean diffusivity; MK, mean kurtosis; FA, fractional anisotropy.

A recent study showed that childhood leukemia survivors with history of cranial radiotherapy had altered diffusion metrics in the fornix, uncinate fasciculus, and cingulum, which are important structures that subserve episodic memory, learning, and attention (22). Leung et al. found significant change in the FA of the posterior thalamic radiation of medulloblastoma survivors after cranial irradiation and chemotherapy (23). We found GCT survivors had significant microstructural changes in these brain regions, as well as in projection fibers such as the corona radiata, posterior thalamic radiation, and superior longitudinal fasciculus. Furthermore, significant changes were detected in the anterior limb of the internal capsule containing projection fibers between the lentiform nucleus and caudate nucleus, which are responsible for the control of motor and sensory pathways.

It is well known that executive function, attention and memory are regulated by deep brain nuclei in the subcortical regions of the brain. We found significant microstructural changes in the grey matter of intracranial GCT survivors. Significant differences were found in the MD of grey matter regions responsible for language, cognition, and executive functions, including the cingulum, amygdala, temporal gyrus, fusiform, and rolandic operculum. Significant differences were also found in brain regions responsible for visual processing, including the calcarine, lingual gyrus, and cuneus. Other affected brain regions included Heschl's gyrus, which is the primary auditory cortex, the precentral gyrus containing the primary motor cortex, and the postcentral gyrus containing the somatosensory cortex.

The estimated FSIQ is typically derived from subtests for performance IQ as well as verbal IQ. Our results showed that the IQ scores were negatively correlated with the MD of brain regions responsible for language processing, including those related to Wernicke's area in the temporal lobe. Heschl's gyrus is associated with the processing of speech-related cues, which facilitates learning and perception of new speech sounds (24). In addition, lower IQ scores were found to be associated with the MD of brain regions responsible for cognitive function such as the hippocampus, parahippocampal gyrus, and anterior cingulum. The frontal regions of the brain are known to be involved in cognitive functions and control of emotions. Our study showed significant association between FSIQ scores and MD values in frontal regions such as the orbitofrontal cortex as well as regions around Broca's area. The frontal inferior opercularis acts indirectly through the motor cortex within the precentral gyrus to control the motor aspects of speech production (25). Interestingly, it is common for patients with neurodegenerative diseases such as Alzheimer's disease and dementia to have motor speech deficits (26, 27). Hence, GCT survivors might be prone to motor speech problems. Our findings are consistent with previous studies on childhood acute lymphoblastic leukemia survivors with a history of chemotherapy and/or radiotherapy, which found that lower volume of the caudate nucleus, was associated with significantly worse verbal fluency (28). In addition, our study demonstrated the significant association of the precentral gyrus with the IQ scores of GCT survivors, suggestive of the involvement of the precentral gyrus in cognitive tasks. The precentral gyrus is the site of the primary motor cortex and is traditionally implicated in voluntary movement control. However, more recent studies suggested that the primary motor cortex not only plays a role in stimulus-response compatibility, plasticity, motor sequence learning and memory as well as learning of sensorimotor associations, but is also engaged in motor imagery, spatial transformations and working memory tasks (29–32). Therefore, our study provides additional evidence to support the involvement of the primary motor cortex in higher cognitive tasks.

Most of the microstructural changes that were associated with functional impairment, as indicated by the poor KPS score, were in white matter regions. These regions included the pyramidal tracts within the internal capsule or fiber tracts such as the corona radiata above the basal ganglia, which had elevated MD but reduced MK and FA. Our findings were consistent with studies on children with cerebral palsy, which found significant correlation between motor function scores and the FA of sensory and motor pathways such as the corticospinal tract, thalamic radiation, or the posterior limb of the internal capsule (33). Functional impairments that were associated with microstructural changes in grey matter regions were mostly confined around the basal ganglia, which have important roles in motor control.

Historically, radiation damage was thought to affect brain white matter rather than the cortex itself (12, 34). Nevertheless, a recent study demonstrated that brain tumor survivors with a history of irradiation had cortical atrophy that was dependent on the radiation dose (35). Seibert et al. showed that cortical atrophy in patients after brain radiotherapy was significantly associated with radiation dose in the entorhinal and inferior parietal regions, which are areas responsible for memory and executive functions (36). They also demonstrated that these cerebral cortex regions seemed to be more vulnerable to dose-dependent radiation atrophy. Our study corroborates the findings by Seibert et al. We also found significant correlations between grey matter microstructural changes and cognitive function in GCT survivors with history of brain radiotherapy. Our study is first to demonstrate significant associations between white and grey matter microstructural changes in vulnerable brain regions of GCT survivors in association with cognitive impairments and/or functional deficits.

Our study had several limitations. First, the number of study subjects was small. Nevertheless, our study was the first to perform DKI measurements in association with cognitive and physical functioning assessments in a cohort of GCT survivors. In addition, our study participants were predominantly male (80%). However, predilection to the male gender is a well-known characteristic of GCT (37) and previous studies also demonstrated similar male: female ratio (38, 39). Second, due to the retrospective nature of the study, we did not have information on the physical or neurocognitive functions in our cohort at the time of tumor diagnosis. Therefore, it is hard to ascertain if the cognitive or functional impairments are due to individual or combined effects of the tumor, chemotherapy, or radiotherapy. Nevertheless, radiation-induced brain damage has long been recognized in pediatric cancer patients, more recent studies have shown that chemotherapy can also lead to neurotoxicity (40). The microstructural brain changes and cognitive or functional impairments that were found in the current study are likely due to the combined effects of all three factors. Lastly,

the measurement of the diffusion metrics of GM regions could be confounded by the partial volume effect from free fluid such as cerebral spinal fluid, for which could not be accounted in our statistical analyses.

In conclusion, our DKI study has successfully demonstrated that impairment in cognitive function and/or deficits in physical functioning were associated with microstructural changes in multiple white and grey matter regions. Proton radiotherapy with reduced irradiation dosage to vulnerable brain regions might lead to improved cognitive and functional outcomes. Diffusion metrics obtained from DKI could potentially be used to identify patients at high risk of cognitive or functional impairment for timely interventions.

DATA AVAILABILITY STATEMENT

The raw data supporting the conclusions of this article will be made available upon request to the authors.

ETHICS STATEMENT

The studies involving human participants were reviewed and approved by The Institutional Review Board of the University of Hong Kong/Hospital Authority Hong Kong West Cluster (HKU/HA HKW IRB), the Research Ethics Committee of the Kowloon Central/ Kowloon East Cluster (KC/KE CREC), Kowloon West Cluster (KW CEREC) and New Territories West Cluster (NTW CEREC). Written informed consent to participate in this study was provided by the participants' legal guardian/next of kin.

AUTHOR CONTRIBUTIONS

Conceptualization: WT, EH, TL, PK and GC. Data curation: WT, EH, TL, AL, PI, VV, KC, DF, DHFC, FH, KY, DK, DKLC, CL, MS, LL, PK and GC. Formal analysis: WT, EH, TL, AL, KC, DF, FH, KY, LL, PK and GC. Funding acquisition: WT. Investigation: WT, EH, TL, VV, PK and GC. Methodology: WT, EH, TL, AL, PI and FH, PK and GC. Project administration: WT, EH, TL, PK and GC. Software: EH and KY. Supervision: WT, EH, TL, PK and GC. Validation: DF. Writing – original draft: WT and EH. Writing – review and editing: WT, EH, TL, AL, PI, VV, KC, DF, DHFC, FH, KY, DK, DKLC, CL, MS, LL, PK and GC. All authors contributed to the article and approved the submitted version.

FUNDING

This work was supported by Research Grants Council of the Hong Kong Special Administrative Region, China (No. HKU 17118815). The funder had no role in the design of the study; the collection, analysis, and interpretation of the data; the writing of the manuscript; and the decision to submit the manuscript for publication.

SUPPLEMENTARY MATERIAL

The Supplementary Material for this article can be found online at: https://www.frontiersin.org/articles/10.3389/fonc.2021.573798/full#supplementary-material

REFERENCES

1. Hodgson KD, Hutchinson AD, Wilson CJ, Nettelbeck T. A Meta-Analysis of the Effects of Chemotherapy on Cognition in Patients With Cancer. *Cancer Treat Rev* (2013) 39(3):297–304. doi: 10.1016/j.ctrv.2012.11.001
2. Sleurs C, Deprez S, Emsell L, Lemiere J, Uyttebroeck A. Chemotherapy-Induced Neurotoxicity in Pediatric Solid Non-CNS Tumor Patients: An Update on Current State of Research and Recommended Future Directions. *Crit Rev Oncol Hematol* (2016) 103:37–48. doi: 10.1016/j.critrevonc.2016.05.001
3. Tso WWY, Liu APY, Lee TMC, Cheuk KL, Shing MK, Luk CW, et al. Neurocognitive Function, Performance Status, and Quality of Life in Pediatric Intracranial Germ Cell Tumor Survivors. *J Neurooncol* (2019) 141(2):393–401. doi: 10.1007/s11060-018-03045-3
4. Liang SY, Yang TF, Chen YW, Liang ML, Chen HH, Chang KP, et al. Neuropsychological Functions and Quality of Life in Survived Patients With Intracranial Germ Cell Tumors After Treatment. *Neuro Oncol* (2013) 15 (11):1543–51. doi: 10.1093/neuonc/not127
5. Quattrocchi CC, Longo D, Delfino LN, Errante Y, Aiello C, Fariello G, et al. MR Differential Diagnosis of Acute Deep Grey Matter Pathology in Paediatric Patients. *Pediatr Radiol* (2013) 43(6):743–61. doi: 10.1007/s00247-012-2491-2
6. Tso WW, Yung AW, Lau HY, Chan GC. Basal Ganglia Germinoma: MRI Classification Correlates Well With Neurological and Cognitive Outcome. *J Pediatr Hematol Oncol* (2014) 36(7):e443–7. doi: 10.1097/MPH.0000000000000014
7. Nagata K, Nikaido Y, Yuasa T, Fujimoto K, Kim YJ, Inoue M. Germinoma Causing Wallerian Degeneration. Case Report and Review of the Literature. *J Neurosurg* (1998) 88(1):126–8. doi: 10.3171/jns.1998.88.1.0126
8. Fouladi M, Chintagumpala M, Laningham FH, Ashley D, Kellie SJ, Langston JW, et al. White Matter Lesions Detected by Magnetic Resonance Imaging After Radiotherapy and High-Dose Chemotherapy in Children With Medulloblastoma or Primitive Neuroectodermal Tumor. *J Clin Oncol* (2004) 22(22):4551–60. doi: 10.1200/JCO.2004.03.058
9. Harila-Saari AH, Paakko EL, Vainionpaa LK, Pyhtinen J, Lanning BM. A Longitudinal Magnetic Resonance Imaging Study of the Brain in Survivors in Childhood Acute Lymphoblastic Leukemia. *Cancer* (1998) 83(12):2608–17. doi: 10.1002/(SICI)1097-0142(19981215)83:12<2608::AID-CNCR28>3.0.CO;2-L
10. Iuvone L, Mariotti P, Colosimo C, Guzzetta F, Ruggiero A, Riccardi R. Long-Term Cognitive Outcome, Brain Computed Tomography Scan, and Magnetic Resonance Imaging in Children Cured for Acute Lymphoblastic Leukemia. *Cancer* (2002) 95(12):2562–70. doi: 10.1002/cncr.10999
11. Peiffer AM, Leyrer CM, Greene-Schloesser DM, Shing E, Kearns WT, Hinson WH, et al. Neuroanatomical Target Theory as a Predictive Model for Radiation-Induced Cognitive Decline. *Neurology* (2013) 80(8):747–53. doi: 10.1212/WNL.0b013e318283bb0a
12. Khong PL, Leung LH, Fung AS, Fong DY, Qiu D, Kwong DL, et al. White Matter Anisotropy in Post-Treatment Childhood Cancer Survivors: Preliminary Evidence of Association With Neurocognitive Function. *J Clin Oncol* (2006) 24(6):884–90. doi: 10.1200/JCO.2005.02.4505
13. Khong PL, Kwong DL, Chan GC, Sham JS, Chan FL, Ooi GC. Diffusion-Tensor Imaging for the Detection and Quantification of Treatment-Induced White Matter Injury in Children With Medulloblastoma: A Pilot Study. *AJNR Am J Neuroradiol* (2003) 24(4):734–40.
14. Lange M, Joly F, Vardy J, Ahles T, Dubois M, Tron L, et al. Cancer-Related Cognitive Impairment: An Update on State of the Art, Detection, and Management Strategies in Cancer Survivors. *Ann Oncol* (2019) 30 (12):1925–40. doi: 10.1093/annonc/mdz410
15. Weber RA, Hui ES, Jensen JH, Nie X, Falangola MF, Helpern JA, et al. Diffusional Kurtosis and Diffusion Tensor Imaging Reveal Different

Time-Sensitive Stroke-Induced Microstructural Changes. *Stroke* (2015) 46 (2):545–50. doi: 10.1161/STROKEAHA.114.006782
16. Guo YL, Zhang ZP, Zhang GS, Kong LM, Rao HB, Chen W, et al. Evaluation of Mean Diffusion and Kurtosis MRI Mismatch in Subacute Ischemic Stroke: Comparison With NIHSS Score. *Brain Res* (2016) 1644:231–9. doi: 10.1016/j.brainres.2016.05.020
17. Grossman EJ, Jensen JH, Babb JS, Chen Q, Tabesh A, Fieremans E, et al. Cognitive Impairment in Mild Traumatic Brain Injury: A Longitudinal Diffusional Kurtosis and Perfusion Imaging Study. *AJNR Am J Neuroradiol* (2013) 34(5):951–7. doi: 10.3174/ajnr.A3358. S1-3.
18. Yuan L, Sun M, Chen Y, Long M, Zhao X, Yin J, et al. Non-Gaussian Diffusion Alterations on Diffusion Kurtosis Imaging in Patients With Early Alzheimer's Disease. *Neurosci Lett* (2016) 616:11–8. doi: 10.1016/j.neulet.2016.01.021
19. Bouffet E, Baranzelli M, Patte C, Portas M, Edan C, Chastagner P, et al. Combined Treatment Modality for Intracranial Germinomas: Results of a Multicentre SFOP Experience. *Br J Cancer* (1999) 79(7-8):1199. doi: 10.1038/sj.bjc.6690192
20. Goldman S, Bouffet E, Fisher PG, Allen JC, Robertson PL, Chuba PJ, et al. Phase II Trial Assessing the Ability of Neoadjuvant Chemotherapy With or Without Second-Look Surgery to Eliminate Measurable Disease for Nongerminomatous Germ Cell Tumors: A Children's Oncology Group Study. *J Clin Oncol* (2015) 33(22):2464. doi: 10.1200/JCO.2014.59.5132
21. Tabesh A, Jensen JH, Ardekani BA, Helpern JA. Estimation of Tensors and Tensor-Derived Measures in Diffusional Kurtosis Imaging. *Magnetic Resonance Med* (2011) 65(3):823–36. doi: 10.1002/mrm.22655
22. Follin C, Svard D, van Westen D, Bjorkman-Burtscher IM, Sundgren PC, Fjalldal S, et al. Microstructural White Matter Alterations Associated to Neurocognitive Deficits in Childhood Leukemia Survivors Treated With Cranial Radiotherapy - a Diffusional Kurtosis Study. *Acta Oncol* (2019) 58 (7):1021–28. doi: 10.1080/0284186X.2019.1571279
23. Leung LH, Ooi GC, Kwong DL, Chan GC, Cao G, Khong PL. White-Matter Diffusion Anisotropy After Chemo-Irradiation: A Statistical Parametric Mapping Study and Histogram Analysis. *Neuroimage* (2004) 21(1):261–68. doi: 10.1016/j.neuroimage.2003.09.020
24. Warrier C, Wong P, Penhune V, Zatorre R, Parrish T, Abrams D, et al. Relating Structure to Function: Heschl's Gyrus and Acoustic Processing. *J Neurosci* (2009) 29(1):61–9. doi: 10.1523/JNEUROSCI.3489-08.2009
25. Nakamichi N, Takamoto K, Nishimaru H, Fujiwara K, Takamura Y, Matsumoto J, et al. Cerebral Hemodynamics in Speech-Related Cortical Areas: Articulation Learning Involves the Inferior Frontal Gyrus, Ventral Sensory-Motor Cortex, and Parietal-Temporal Sylvian Area. *Front Neurol* (2018) 9:939. doi: 10.3389/fneur.2018.00939
26. Poole ML, Brodtmann A, Darby D, Vogel AP. Motor Speech Phenotypes of Frontotemporal Dementia, Primary Progressive Aphasia, and Progressive Apraxia of Speech. *J Speech Lang Hear Res* (2017) 60(4):897–911. doi: 10.1044/2016_JSLHR-S-16-0140
27. Cera ML, Ortiz KZ, Bertolucci PH, Minett TS. Speech and Orofacial Apraxias in Alzheimer's Disease. *Int Psychogeriatr* (2013) 25(10):1679–85. doi: 10.1017/S1041610213000781
28. Zajac-Spychala O, Pawlak MA, Karmelita-Katulska K, Pilarczyk J, Derwich K, Wachowiak J. Long-Term Brain Structural Magnetic Resonance Imaging and Cognitive Functioning in Children Treated for Acute Lymphoblastic Leukemia With High-Dose Methotrexate Chemotherapy Alone or Combined With CNS Radiotherapy At Reduced Total Dose to 12 Gy. *Neuroradiology* (2017) 59(2):147–56. doi: 10.1007/s00234-016-1777-8
29. Tomasino B, Gremese M. The Cognitive Side of M1. *Front Hum Neurosci* (2016) 10:298. doi: 10.3389/fnhum.2016.00298
30. Kaas AL, van Mier H, Goebel R. The Neural Correlates of Human Working Memory for Haptically Explored Object Orientations. *Cereb Cortex* (2007) 17 (7):1637–49. doi: 10.1093/cercor/bhl074
31. Porro CA, Francescato MP, Cettolo V, Diamond ME, Baraldi P, Zuiani C, et al. Primary Motor and Sensory Cortex Activation During Motor Performance and Motor Imagery: A Functional Magnetic Resonance Imaging Study. *J Neurosci* (1996) 16(23):7688–98. doi: 10.1523/JNEUROSCI.16-23-07688.1996
32. Kosslyn SM, Thompson WL, Wraga M, Alpert NM. Imagining Rotation by Endogenous Versus Exogenous Forces: Distinct Neural Mechanisms. *Neuroreport* (2001) 12(11):2519–25. doi: 10.1097/00001756-200108080-00046
33. Jiang H, Liu H, He H, Yang J, Liu Z, Huang T, et al. Specific White Matter Lesions Related to Motor Dysfunction in Spastic Cerebral Palsy: A Meta-Analysis of Diffusion Tensor Imaging Studies. *J Child Neurol* (2020) 35 (2):146–54. doi: 10.1177/0883073819879844
34. Qiu D, Kwong DL, Chan GC, Leung LH, Khong PL. Diffusion Tensor Magnetic Resonance Imaging Finding of Discrepant Fractional Anisotropy Between the Frontal and Parietal Lobes After Whole-Brain Irradiation in Childhood Medulloblastoma Survivors: Reflection of Regional White Matter Radiosensitivity? *Int J Radiat Oncol Biol Phys* (2007) 69(3):846–51. doi: 10.1016/j.ijrobp.2007.04.041
35. Karunamuni R, Bartsch H, White NS, Moiseenko V, Carmona R, Marshall DC, et al. Dose-Dependent Cortical Thinning After Partial Brain Irradiation in High-Grade Glioma. *Int J Radiat Oncol Biol Phys* (2016) 94(2):297–304. doi: 10.1016/j.ijrobp.2015.10.026
36. Seibert TM, Karunamuni R, Kaifi S, Burkeen J, Connor M, Krishnan AP, et al. Cerebral Cortex Regions Selectively Vulnerable to Radiation Dose-Dependent Atrophy. *Int J Radiat Oncol Biol Phys* (2017) 97(5):910–18. doi: 10.1016/j.ijrobp.2017.01.005
37. Phi JH, Wang KC, Kim SK. Intracranial Germ Cell Tumor in the Molecular Era. *J Kor Neurosurg Soc* (2018) 61(3):333–42. doi: 10.3340/jkns.2018.0056
38. Takami H, Perry A, Graffeo CS, Giannini C, Narita Y, Nakazato Y, et al. Comparison on Epidemiology, Tumor Location, Histology, and Prognosis of Intracranial Germ Cell Tumors Between Mayo Clinic and Japanese Consortium Cohorts. *J Neurosurg* (2021) 134(2):446–56. doi: 10.3171/2019.11.JNS191576
39. McCarthy BJ, Shibui S, Kayama T, Miyaoka E, Narita Y, Murakami M, et al. Primary CNS Germ Cell Tumors in Japan and the United States: An Analysis of 4 Tumor Registries. *Neuro Oncol* (2012) 14(9):1194–200. doi: 10.1093/neuonc/nos155
40. Dietrich J, Prust M, Kaiser J. Chemotherapy, Cognitive Impairment and Hippocampal Toxicity. *Neuroscience* (2015) 309:224–32. doi: 10.1016/j.neuroscience.2015.06.016

Conflict of Interest: The authors declare that the research was conducted in the absence of any commercial or financial relationships that could be construed as a potential conflict of interest.